SEMARAK ILMU PUBLISHING

Journal of Advanced Research in Fluid Mechanics and Thermal Sciences

Journal homepage:
https://semarakilmu.com.my/journals/index.php/fluid_mechanics_thermal_sciences/index
ISSN: 2289-7879

Numerical Investigation of Ferrofluid Flow at Lower Stagnation Point over a Solid Sphere using Keller-Box Method

Siti Hanani Mat Yasin[1], Muhammad Khairul Anuar Mohamed[1], Zulkhibri Ismail[1], Basuki Widodo[2], Mohd Zuki Salleh[1,*]

[1] Centre for Mathematical Sciences, College of Computing and Applied Sciences, Universiti Malaysia Pahang, Lebuhraya Tun Razak, 26300 Gambang, Kuantan, Pahang, Malaysia
[2] Department of Mathematics, Institut Teknologi Sepuluh Nopember, 60111 Surabaya, Indonesia

ARTICLE INFO

Article history:
Received 3 January 2022
Received in revised form 23 March 2022
Accepted 25 March 2022
Available online 29 April 2022

Keywords:
Ferrofluid; solid sphere; magnetohydrodynamic; magnetite

ABSTRACT

In this paper, ferrofluid flow at lower stagnation point on solid sphere is investigated theoretically by considering mixed convection boundary layer flow. The sphere surface is exposed to the magnetic field and thermal radiation by taking into account constant wall temperature boundary conditions. The discovery of the existing magnetic field near the surface while the ferrofluid flowing leads to the development of phenomenology called magnetohydrodynamic. The magnetite (Fe_3O_4) acts as nanoparticles dispersant and suspended in the water contained in ferrofluid are assumed as Newtonian fluid and behave as single-phase fluid flow is studied. These assumptions give physical insight into the behaviour of ferrofluid flow to be analysed and discussed. The Keller-box method is applied to solve the transformed partial differential equations numerically. The numerical results found the viscosity measured from magnetite (Fe_3O_4) volume fraction is the main element provided to the trend of the ferrofluid velocity flow. Besides, the ferrofluid temperature at lower stagnation point on sphere is proven influence the ferrofluid viscosity and change the velocity of ferrofluid flow.

1. Introduction

Nowadays, the research of nanofluids is growing faster along with thriving technology. The good outcome of nanofluid as liquids for the cooling system and thermal transport mechanism significantly enhance the thermal conductivity provides compatibility of the heat transfer in wide applications. The study of nanofluid flow and heat transfer requirement as a coolant for forward-looking applications and devices is a vital aspect to contributed the nanofluid in common criteria such as high thermal conductivity, low viscosity, low corrosivity, low toxicity and have thermal stability. The implementation of the experiment study is needed the much time and costly. Therefore, researchers had alternatively using theoretical study with consideration the mathematical approach. The Navier-Stokes equation is a mathematical description of the

[*] *Corresponding author.*
E-mail address: zuki@ump.edu.my

https://doi.org/10.37934/arfmts.94.2.200214

incompressible fluid movement. Nevertheless, it is very complex to solve as it is an elliptical form and have a drawback in applied the viscous flow effect [1]. In 1904, Ludwig Prandtl introduced the concept of boundary layer theory were to highlight the importance of viscosity at the boundary layer region and give a breakthrough in reducing the mathematical difficulty. In the mathematical approach, some problems can be solved using analytical or numerical methods. The mathematical study in fluid flow and heat transfer problems for bluff body geometries is difficult to solve using the analytical method. Consequently, the numerical method is applied to solve the simplification of boundary layer equations.

Further, the nanofluid with magnetic nanoparticles such as magnetite, Fe_3O_4 suspended in a base fluid is known as ferrofluid with the presence of an external magnetic field have been found most sufficient in practice and widely investigated. Ferrofluid is not found in nature but must be synthesized using ball mailing, co-precipitation, decomposition of metal carbonyl and several other methods [2] and exhibits superparamagnetism when exposed to the magnetic field [3]. The benefits of ferrofluid as thermal transfer, voice coil centering, reduction of power compression and damping are indispensable tools for the improvement of loudspeakers audio [4,5]. Meanwhile, ferrofluid is also used in many areas, for example in bio-medical, domain detection and education art [6]. The various applications and advantages of ferrofluid attracted researchers to study the flow and heat transfer of ferrofluid using experiments [7–10] or theoretical methods [11–15]. According to Darus [16], the fluid and heat transfer behaviour shows different outcomes when flows at different geometries. Moreover, the fluid movement over a bluff body such as cylinder and sphere because the boundary layer separation could occur at a certain angle of geometry.

There are two fluid flow and convective heat transfer models of nanofluid which have been frequently used by the researchers namely the Buongiorno model [17] and Tiwari and Das model [18]. Buongiorno model or namely the two-phase model studies the slip mechanism that can produce a relative (slip) velocity between nanoparticles and base fluid. The major findings in his model are based on two velocity slip effect namely Brownion diffusion and thermophoresis. In contrast to Buongiorno model, Tiwari and Das model which is also known as single-phase model stated that the base fluid and nanoparticles are in thermal equilibrium with the same velocity of flow. It also needs to take the solid volume fraction of nanoparticles into account in order to analyse the behaviour of nanofluid using the thermophysical properties values of both base fluid and nanoparticles. The studies related to the used Tiwari and Das model have been conducted by [13,19,20] and other researchers to investigate the ferrofluid flow and heat transfer on the various geometry surface. Unfortunately, most of the studies considered the flat plate and a few researchers explored the fluid flow over the bluff body. It is worthy of note that this study interest is fluid flow at a lower stagnation point on a solid sphere using Tiwari and das model.

2. Mathematical Formulation

Consider the incompressible ferrofluid flow with magnetohydrodynamic effect are steady, two-dimensional and laminar mixed convection boundary layer flow at the lower stagnation point on a solid sphere where uniform transverse magnetic strength, B_o applied perpendicular to the surface. It is assumed the magnetic Reynolds number to be small, thus the induced magnetic field can be neglected compared to the applied magnetic field. Figure 1 illustrated the orthogonal coordinates of $\bar{x}$ is measured along a solid sphere surface and $\bar{y}$ measures the distance normal to the sphere surface with radius, a. Besides, the sphere surface heated to a constant temperature, T_w and exposed to thermal radiation with ambient temperature, T_∞.

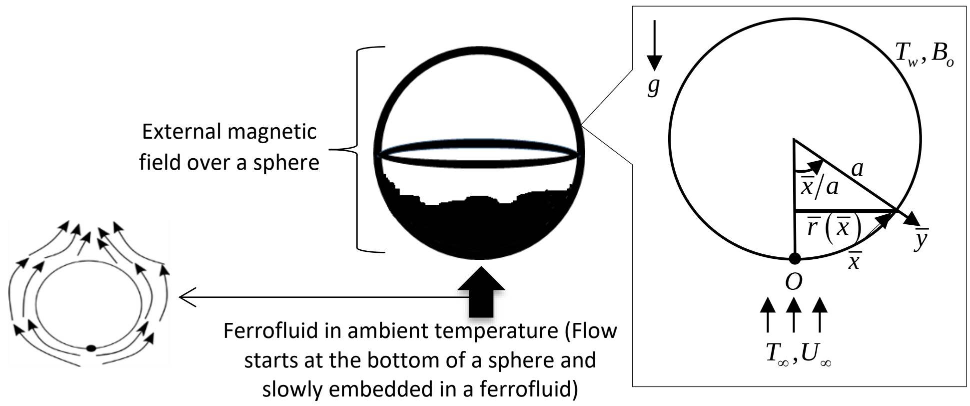

Fig. 1. Physical model and coordinate system

Under the Boussinesq approximation and the assumption of boundary layer approximation, the dimensional governing equations as adopted by [21] as follows

$$\frac{\partial}{\partial \bar{x}}(\bar{r}\bar{u}) + \frac{\partial}{\partial \bar{y}}(\bar{r}\bar{v}) = 0, \tag{1}$$

$$\bar{u}\frac{\partial \bar{u}}{\partial \bar{x}} + \bar{v}\frac{\partial \bar{u}}{\partial \bar{y}} = \bar{u}_e\frac{\partial \bar{u}_e}{\partial \bar{x}} + \nu_{ff}\frac{\partial^2 \bar{u}}{\partial \bar{y}^2} + \frac{(\rho\beta)_{ff}}{\rho_{ff}} g\left(T - T_\infty\right)\sin\frac{\bar{x}}{a} - \frac{\sigma_{ff} B_o^2}{\rho_{ff}}\left(\bar{u} - \bar{u}_e\right), \tag{2}$$

$$\bar{u}\frac{\partial T}{\partial \bar{x}} + \bar{v}\frac{\partial T}{\partial \bar{y}} = \alpha_{ff}\frac{\partial^2 T}{\partial \bar{y}^2} - \frac{1}{\left(\rho C_p\right)_{ff}}\frac{\partial q_r}{\partial \bar{y}}, \tag{3}$$

subject to the boundary conditions

$$\begin{aligned} &\bar{u}(\bar{x},0) = 0,\ \bar{v}(\bar{x},0) = 0,\ T(\bar{x},0) = T_w \ \text{ at } \bar{y} = 0, \\ &\bar{u}(\bar{x},\infty) \to \bar{u}_e(\bar{x}),\ T(\bar{x},\infty) \to T_\infty \ \text{ as } \bar{y} \to \infty, \end{aligned} \tag{4}$$

where $\bar{u}$ and $\bar{v}$ denotes the velocity components along the $\bar{x}$ and $\bar{y}$ axes, respectively. The radial distance from the symmetrical axis and external velocity defined as $\bar{r}\left(\bar{x}\right) = a\sin\left(\bar{x}/a\right)$ and $\bar{u}_e\left(\bar{x}\right) = U_\infty \sin\left(\bar{x}/a\right)$, respectively. Suppose β is to thermal expansion, g is the gravity acceleration and T is ferrofluid temperature. Further, the effective thermophysical properties of ferrofluid (subscript ff) can be defined as

$$\mu_{ff} = \mu_f \big/ (1-\phi)^{2.5}, \nu_{ff} = \mu_{ff} / \rho_{ff}, \alpha_{ff} = k_{ff} \Big/ \rho_{ff} \left(C_p\right)_{ff}, \rho_{ff} = (1-\phi)\rho_f + \phi\rho_s,$$
$$\left(\rho\beta\right)_{ff} = (1-\phi)\left(\rho\beta\right)_f + \phi\left(\rho\beta\right)_s, \left(\rho C_p\right)_{ff} = (1-\phi)\left(\rho C_p\right)_f + \phi\left(\rho C_p\right)_s, \tag{5}$$
$$\frac{\sigma_{ff}}{\sigma_f} = 1 + \frac{3\left(\sigma_s/\sigma_f - 1\right)\phi}{\left(\sigma_s/\sigma_f + 2\right) - \left(\sigma_s/\sigma_f - 1\right)\phi}, \frac{k_{ff}}{k_f} = \frac{k_s + 2k_f - 2\phi(k_f - k_s)}{k_s + 2k_f + \phi(k_f - k_s)},$$

where subscript s and subscript f are ferroparticles and base fluid. Here, the thermophysical properties $\mu, \nu, \alpha, \rho, \rho\beta, \rho C_p, \sigma$ and k represents the dynamic viscosity, kinematic viscosity, thermal diffusivity, effective density, buoyancy coefficient, effective heat capacity, electrical conductivity and thermal conductivity as presented in Table 1.

Table 1
Thermophysical properties of base fluid and ferroparticles [22,23]

Physical Properties	Water	Magnetite(Fe_3O_4)
$\rho\left(\mathrm{kg}\cdot\mathrm{m}^{-3}\right)$	997.1	5200
$C_p\left(\mathrm{J}\cdot\mathrm{kg}^{-1}\cdot\mathrm{K}^{-1}\right)$	4179	670
$k\left(\mathrm{W}\cdot\mathrm{m}^{-1}\cdot\mathrm{K}^{-1}\right)$	0.613	6
$\sigma\left(\Omega\cdot\mathrm{m}\right)^{-1}$	0.05	25000
$\beta\left(\mathrm{K}\right)^{-1}$	21×10^{-5}	1.18×10^{-5}

The Eq. (3) simplified as follows by the Rosseland approximation

$$\bar{u}\frac{\partial T}{\partial \bar{x}} + \bar{v}\frac{\partial T}{\partial \bar{y}} = \alpha_{ff}\frac{\partial^2 T}{\partial \bar{y}^2} + \frac{1}{\left(\rho C_p\right)_{ff}}\frac{16\sigma^* T_\infty^3}{3k^*}\frac{\partial^2 T}{\partial \bar{y}^2}. \tag{6}$$

where the radiative heat flux q_r is defined as

$$q_r = -\frac{4\sigma^*}{3k^*}\frac{\partial T^4}{\partial \bar{y}}, \tag{7}$$

where $\sigma*$ and $k*$ are the Stefan-Boltzmann constant and the mean absorption coefficient, respectively. Introducing the following dimensionless variables as follows to transformed Eq. (1), (2), (4) and (6):

$$r = \bar{r}/a, \quad x = \bar{x}/a, \; y = \mathrm{Re}_x^{1/2}\left(\bar{y}/a\right), \; u = \bar{u}/U_\infty,$$
$$v = \mathrm{Re}_x^{1/2}\left(\bar{v}/U_\infty\right), u_e\left(x\right) = \bar{u}_e\left(x\right)/U_\infty, \quad \theta(\eta) = \left(T - T_\infty\right)/\left(T_w - T_\infty\right), \tag{8}$$

where θ is the rescaled dimensionless temperature of the ferrofluid and $\mathrm{Re}_x = U_\infty a/\nu_f$ is the local Reynolds number. Then, the Eq. (1), (2), (4) and (6) becomes

$$\frac{\partial}{\partial x}\left(ru\right)+\frac{\partial}{\partial y}\left(rv\right)=0, \tag{9}$$

$$u\frac{\partial u}{\partial x}+v\frac{\partial u}{\partial y}=u_e\frac{\partial u_e}{\partial x}+\frac{\mu_{ff}}{\rho_{ff}\nu_f}\frac{\partial^2 u}{\partial y^2}+\frac{(1-\phi)\rho_f+\phi\left(\rho\beta\right)_s/\beta_f}{(1-\phi)\rho_f+\phi\rho_s}\lambda\theta\sin x-\frac{\sigma_{ff}}{\sigma_f}\frac{\rho_f}{\rho_{ff}}M\left(u-u_e\right), \tag{10}$$

$$u\frac{\partial\theta}{\partial x}+v\frac{\partial\theta}{\partial y}=\frac{1}{\Pr}\frac{\left(\rho C_p\right)_f}{\left(\rho C_p\right)_{ff}}\left(\frac{k_{ff}}{k_f}+\frac{4}{3}Nr\right)\frac{\partial^2\theta}{\partial y^2}, \tag{11}$$

subject to the boundary conditions

$$\begin{aligned}&u(x,0)=0,\ v(x,0)=0,\ \theta(x,0)=1,\\&u(x,\infty)\to u_e,\ \ \theta(x,\infty)\to 0,\end{aligned} \tag{12}$$

where the mixed convection parameter, the Grashof number, the magnetic parameter, the Prandtl number and radiation parameter are expressed as

$$\lambda=\frac{Gr_x}{\mathrm{Re}_x^2},\quad Gr_x=\frac{(g\beta_f\left(T_w-T_\infty\right)a^3)}{\nu_f^2},\quad M=\frac{\sigma_f a^2 B_o{}^2(x)}{\mu_f\,\mathrm{Re}},\quad \Pr=\frac{\nu_f\left(\rho C_p\right)_f}{k_f},\quad Nr=\frac{4\sigma^* T_\infty^3}{k^* k_f}. \tag{13}$$

In order to solve the Eq. (9) – (11) subjected to the boundary conditions (12) the functions below is introduced

$$\psi=xr\left(x\right)f(x,y),\quad \theta=\theta(x,y), \tag{14}$$

where ψ is the stream function defined as $u=\left(1/r\right)\left(\partial\psi/\partial y\right)$ and $v=-\left(1/r\right)\left(\partial\psi/\partial x\right)$ which satisfies Eq. (9) and the Eq. (10) and Eq. (11) are obtained

$$\begin{aligned}&\frac{1}{(1-\phi)^{2.5}\left[1-\phi+(\phi\rho_s)/(\rho_f)\right]}\left(\frac{\partial^3 f}{\partial y^3}\right)+\left(1+\frac{x}{\sin x}\cos x\right)\left(f\frac{\partial^2 f}{\partial y^2}\right)-\left(\frac{\partial f}{\partial y}\right)^2+\\&\left(\frac{9}{4}\cos x+\frac{(1-\phi)\rho_f+\phi\left(\rho\beta\right)_s/\beta_f}{(1-\phi)\rho_f+\phi\rho_s}\lambda\theta\right)\left(\frac{\sin x}{x}\right)-\frac{\sigma_{ff}/\sigma_f}{\left(1-\phi\right)+\phi\left(\rho_s/\rho_f\right)}M\left(\frac{\partial f}{\partial y}-\frac{3}{2}\frac{\sin x}{x}\right)=\\&x\left(\frac{\partial f}{\partial y}\frac{\partial^2 f}{\partial x\partial y}-\frac{\partial f}{\partial x}\frac{\partial^2 f}{\partial y^2}\right),\end{aligned} \tag{15}$$

$$\frac{1}{\Pr}\frac{\left(\rho C_p\right)_f}{\left(\rho C_p\right)_{ff}}\left(\frac{k_{ff}}{k_f}+\frac{4}{3}Nr\right)\frac{\partial^2\theta}{\partial y^2}+\left(1+\frac{x}{\sin x}\cos x\right)f\frac{\partial\theta}{\partial y}=x\left(\frac{\partial f}{\partial y}\frac{\partial\theta}{\partial x}-\frac{\partial f}{\partial x}\frac{\partial\theta}{\partial y}\right), \tag{16}$$

subject to the boundary conditions

$$f(x,0)=0,\quad \frac{\partial f}{\partial y}(x,0)=0,\quad \theta(x,0)=1,$$
$$\frac{\partial f}{\partial y}(x,\infty)\to\frac{3}{2}\frac{\sin x}{x},\quad \theta(x,\infty)\to 0. \tag{17}$$

It should be emphasized that the position of ferrofluid flow at the lower stagnation point of a solid sphere occur when $x\approx 0$. Thus, the Eq. (15) and Eq. (16) subjected to the boundary conditions (17) will be reduced to the following ordinary differential equations that the f' and θ' denotes the differentiation with respect to the variable y

$$\frac{1}{(1-\phi)^{2.5}\left[1-\phi+(\phi\rho_s)/(\rho_f)\right]}f'''+2ff''-f'^2+\frac{(1-\phi)\rho_f+\phi\left(\rho\beta\right)_s/\beta_f}{(1-\phi)\rho_f+\phi\rho_s}\lambda\theta+\frac{9}{4}$$
$$-\frac{\sigma_{ff}/\sigma_f}{\left(1-\phi\right)+\phi\left(\rho_s/\rho_f\right)}M\left(f'-\frac{3}{2}\right)=0, \tag{18}$$

$$\frac{1}{\Pr}\frac{\left(\rho C_p\right)_f}{\left(\rho C_p\right)_{ff}}\left(\frac{k_{ff}}{k_f}+\frac{4}{3}Nr\right)\theta''+2f\theta'=0, \tag{19}$$

and the boundary conditions

$$f(0)=0,\quad f'(0)=0,\quad \theta(0)=1,$$
$$f'(\infty)\to\frac{3}{2},\quad \theta(\infty)\to 0. \tag{20}$$

The local Nusselt number of the ferrofluid can be expressed as

$$Nu_x=\frac{aq_w}{k_f(T_w-T_\infty)}\qquad \text{where}\qquad q_w=-k_{ff}\left(\frac{\partial T}{\partial\bar{y}}\right)_{\bar{y}=0}+q_r, \tag{21}$$

then transform into the dimensionless form using the variable in Eq. (8) become

$$Nu_xGr^{-1/4}=-\left(\frac{k_{ff}}{k_f}+\frac{4}{3}Nr\right)\frac{\partial\theta}{\partial y}\left(x,0\right). \tag{22}$$

The velocity profiles and temperature distributions at the lower stagnation point of a solid sphere can be obtained from the following relations

$$u=f'(y)\ \text{and}\ \theta=\theta(y). \tag{23}$$

3. Keller-box Method

Keller-box methods start with transform the Eq. (15) and Eq. (16) subjected to the boundary conditions (17) into the first-order system using the following dependent variables

$$f' = u,\ u' = v,\ s' = t. \tag{24}$$

Then the equations becomes

$$\begin{gathered}(\mathrm{aa})v' + \left(1 + \frac{x}{\sin x}\cos x\right) fv - (u)^2 + \left(\frac{9}{4}\cos x + (\mathrm{ab})\lambda s\right)\left(\frac{\sin x}{x}\right) - (\mathrm{ac})M\left(u - \frac{3}{2}\frac{\sin x}{x}\right) = \\ x\left(u\frac{\partial u}{\partial x} - v\frac{\partial f}{\partial x}\right),\end{gathered} \tag{25}$$

$$\frac{1}{\mathrm{Pr}}(\mathrm{ad})\left((\mathrm{ae}) + \frac{4}{3}Nr\right)t' + \left(1 + \frac{x}{\sin x}\cos x\right) ft = x\left(u\frac{\partial s}{\partial x} - t\frac{\partial f}{\partial x}\right), \tag{26}$$

with boundary conditions

$$\begin{gathered}f(x,0) = 0, \quad u(x,0) = 0, \quad s(x,0) = 1, \\ u(x,\infty) \to \frac{3}{2}\frac{\sin x}{x}, \quad s(x,\infty) \to 0.\end{gathered} \tag{27}$$

where $f = f(y), \theta = s(y)$ and $(')$ is derivative respect to y with let

$$\mathrm{aa} = \frac{1}{(1-\phi)^{2.5}\left[1 - \phi + (\phi\rho_s)/(\rho_f)\right]},\ \mathrm{ab} = \frac{(1-\phi)\rho_f + \phi(\rho\beta)_s/\beta_f}{(1-\phi)\rho_f + \phi\rho_s},\ \mathrm{ac} = \frac{\sigma_{ff}/\sigma_f}{(1-\phi) + \phi(\rho_s/\rho_f)},$$
$$\mathrm{ad} = \frac{(\rho C_p)_f}{(\rho C_p)_{ff}},\ \mathrm{ae} = \frac{k_{ff}}{k_f}.$$

The Eq. (24) – (26) are written in finite difference by using central differences with considering rectangle mesh points as [24]. Thus we get

$$\frac{f_j^n - f_{j-1}^n}{h_j} = \frac{u_j^n + u_{j-1}^n}{2} = u_{j-1/2}^n, \quad \frac{u_j^n - u_{j-1}^n}{h_j} = \frac{v_j^n + v_{j-1}^n}{2} = \mathrm{v}_{j-1/2}^n, \quad \frac{s_j^n - s_{j-1}^n}{h_j} = \frac{t_j^n + t_{j-1}^n}{2} = t_{j-1/2}^n, \tag{28}$$

$$\begin{gathered}(\mathrm{aa})\frac{v_j^n - v_{j-1}^n}{h_j} + (E+\alpha) f_{j-1/2}^n v_{j-1/2}^n - (1+\alpha)(u^2)_{j-1/2}^n + \frac{9}{4}A + (\mathrm{ab})\lambda B s_{j-1/2}^n - \\ (\mathrm{ac})M\left(u_{j-1/2}^n - \frac{3}{2}\mathrm{B}\right) + \alpha f_{j-1/2}^n v_{j-1/2}^{n-1} - \alpha f_{j-1/2}^{n-1} v_{j-1/2}^n = \left[-L_1 + \alpha fv - \alpha u^2\right]_{j-1/2}^{n-1},\end{gathered} \tag{29}$$

$$\frac{1}{\Pr}(\mathrm{ad})\left((\mathrm{ae})+\frac{4}{3}\mathrm{Nr}\right)\frac{t_j^n-t_{j-1}^n}{h_j}+(E+\alpha)f_{j-1/2}^n t_{j-1/2}^n-\alpha u_{j-1/2}^n s_{j-1/2}^n-\alpha u_{j-1/2}^{n-1}s_{j-1/2}^n+$$
$$\alpha u_{j-1/2}^n s_{j-1/2}^{n-1}-\alpha f_{j-1/2}^{n-1}t_{j-1/2}^n+\alpha f_{j-1/2}^n t_{j-1/2}^{n-1}=\left[-L_2-\alpha us+\alpha ft\right]_{j-1/2}^{n-1}, \tag{30}$$

with boundary conditions

$$f_0^n=0,\ u_0^n=0,\ s_0^n=1,\ u_J^n=\frac{3}{2}B,\ s_J^n=0, \tag{31}$$

where

$$\alpha=\frac{x^{n-1/2}}{k_n},\quad B=\frac{\sin x^{n-1/2}}{x^{n-1/2}},\quad E=1+\left(x^{n-1/2}\right)\left(\cot x^{n-1/2}\right),\quad A=\left(\cos x^{n-1/2}\right)(B),$$
$$(L_1)_{j-1/2}^{n-1}=\left[(\mathrm{aa})\frac{v_j-v_{j-1}}{h_j}+Ef_{j-1/2}\,v_{j-1/2}-\left(u_{j-1/2}\right)^2+\frac{9}{4}A+(ab)\lambda Bs_{j-1/2}-(ac)M\left(u_{j-1/2}-B\right)\right]^{n-1},$$
$$(L_2)_{j-1/2}^{n-1}=\left[\frac{1}{\Pr}(ad)\left((ae)+\frac{4}{3}Nr\right)\frac{t_j-t_{j-1}}{h_j}+Ef_{j-1/2}\,t_{j-1/2}\right]^{n-1}.$$

Next, the equations are linearized by Newton's method. The following iterates are introduced:

$$f_j^{(i+1)}=f_j^{(i)}+\delta f_j^{(i)},u_j^{(i+1)}=u_j^{(i)}+\delta u_j^{(i)},v_j^{(i+1)}=v_j^{(i)}+\delta v_j^{(i)},s_j^{(i+1)}=s_j^{(i)}+\delta s_j^{(i)},t_j^{(i+1)}=t_j^{(i)}+\delta t_j^{(i)}, \tag{32}$$

then substitute in the Eq. (28) – (30) and eliminated the superscript along with the higher order of δ as follows:

$$\delta f_j-\delta f_{j-1}-\frac{1}{2}h_j\left(\delta u_j+\delta u_{j-1}\right)=(r_1)_{j-1/2},$$
$$\delta u_j-\delta u_{j-1}-\frac{1}{2}h_j\left(\delta v_j+\delta v_{j-1}\right)=(r_2)_{j-1/2}, \tag{33}$$
$$\delta s_j-\delta s_{j-1}-\frac{1}{2}h_j\left(\delta t_j+\delta t_{j-1}\right)=(r_3)_{j-1/2},$$

$$(a_1)_j\delta v_j+(a_2)_j\delta v_{j-1}+(a_3)_j\delta f_j+(a_4)_j\delta f_{j-1}+(a_5)_j\delta u_j+(a_6)_j\delta u_{j-1}+(a_7)_j\delta s_j+$$
$$(a_8)_j\delta s_{j-1}=(r_4)_{j-1/2}, \tag{34}$$

$$(b_1)_j\delta t_j+(b_2)_j\delta t_{j-1}+(b_3)_j\delta f_j+(b_4)_j\delta f_{j-1}+(b_5)_j\delta s_j+(b_6)_j\delta s_{j-1}+(b_7)_j\delta u_j+$$
$$(b_8)_j\delta u_{j-1}=(r_5)_{j-1/2}, \tag{35}$$

where

$$(a_1)_j = (\mathrm{aa}) + \frac{h_j(E+\alpha)}{2} f_{j-1/2} - \frac{h_j\alpha}{2} f_{j-1/2}^{n-1},$$
$$(a_2)_j = (a_1)_j - 2(\mathrm{aa}),$$
$$(a_3)_j = \frac{h_j(E+\alpha)}{2} v_{j-1/2} + \frac{h_j\alpha}{2} v_{j-1/2}^{n-1},$$
$$(a_4)_j = (a_3)_j,$$
$$(a_5)_j = -h_j(1+\alpha)u_{j-1/2} - \frac{h_j(\mathrm{ac})M}{2},$$
$$(a_6)_j = (a_5)_j,$$
$$(a_7)_j = \frac{h_j(\mathrm{ab})\lambda B}{2},$$
$$(a_8)_j = (a_7)_j,$$

$$(b_1)_j = \frac{1}{\Pr}(\mathrm{ad})\left((\mathrm{ae}) + \frac{4}{3}Nr\right) + \frac{h_j(E+\alpha)}{2} f_{j-1/2} - \frac{h_j\alpha}{2} f_{j-1/2}^{n-1},$$
$$(b_2)_j = (b_1)_j - 2\left(\frac{1}{\Pr}(\mathrm{ad})\left((\mathrm{ae}) + \frac{4}{3}Nr\right)\right),$$
$$(b_3)_j = \frac{h_j(E+\alpha)}{2} t_{j-1/2} + \frac{h_j\alpha}{2} t_{j-1/2}^{n-1},$$
$$(b_4)_j = (b_3)_j,$$
$$(b_5)_j = -\frac{h_j\alpha}{2} u_{j-1/2} - \frac{h_j\alpha}{2} u_{j-1/2}^{n-1},$$
$$(b_6)_j = (b_5)_j,$$
$$(b_7)_j = -\frac{h_j\alpha}{2} s_{j-1/2} + \frac{h_j\alpha}{2} s_{j-1/2}^{n-1},$$
$$(b_8)_j = (b_7)_j,$$

$$(r_1)_{j-1/2} = f_{j-1} - f_j + h_j u_{j-1/2},$$
$$(r_2)_{j-1/2} = u_{j-1} - u_j + h_j v_{j-1/2},$$
$$(r_3)_{j-1/2} = s_{j-1} - s_j + h_j t_{j-1/2},$$
$$(r_4)_{j-1/2} = aa\left(-v_j + v_{j-1}\right) - h_j\left(E+\alpha\right) f_{j-1/2} v_{j-1/2} + h_j\left(1+\alpha\right)\left(u_{j-1/2}\right)^2 - h_j \frac{9}{4} A$$
$$- h_j (ab)\lambda B s_{j-1/2} + h_j\left(\mathrm{ac}\right) M\left(u_{j-1/2} - \frac{3}{2}B\right) - h_j \alpha f_{j-1/2} v_{j-1/2}^{n-1} + h_j \alpha v_{j-1/2} f_{j-1/2}^{n-1} + \left(R_1\right)_{j-1/2}^{n-1},$$
$$(r_5)_{j-1/2} = \frac{1}{\mathrm{Pr}}\left(\mathrm{ad}\right)\left(\left(\mathrm{ae}\right) + \frac{4}{3}Nr\right)\left(-t_j + t_{j-1}\right) - h_j\left(E+\alpha\right) f_{j-1/2} t_{j-1/2} + h_j \alpha u_{j-1/2} s_{j-1/2}$$
$$- h_j \alpha u_{j-1/2} s_{j-1/2}^{n-1} + h_j \alpha s_{j-1/2} u_{j-1/2}^{n-1} + h_j \alpha t_{j-1/2} f_{j-1/2}^{n-1} - h_j \alpha f_{j-1/2} t_{j-1/2}^{n-1} + \left(R_2\right)_{j-1/2}^{n-1},$$

with $\left(R_1\right)_{j-1/2}^{n-1} = h_j\left[-L_1 + \alpha f v - \alpha u^2\right]_{j-1/2}^{n-1}$ and $\left(R_2\right)_{j-1/2}^{n-1} = h_j\left[-L_2 - \alpha u s + \alpha f t\right]_{j-1/2}^{n-1}$.

The linear equations system (33) – (35) satisfied exactly with no iteration and the correct values maintain in all iterates when let

$$\delta f_0 = 0,\ \delta u_0 = 0,\ \delta s_0 = 0,\ ,\ \delta u_J = 0 \text{ and } \delta s_J = 0 \tag{36}$$

The linear equations system (33) – (35) solved by using the block elimination technique in matrix-vector form when $j = 1, \ldots, J$ as follow

$$\mathrm{A}\delta = \mathrm{r}, \tag{37}$$

with

$$\mathrm{A} = \begin{bmatrix} [A_1] & [C_1] & & & & \\ [B_2] & [A_2] & [C_2] & & & \\ & & \ddots & & & \\ & & \ddots & & & \\ & & \ddots & & & \\ & & & [B_{J-1}] & [A_{J-1}] & [C_{J-1}] \\ & & & & [B_J] & [A_J] \end{bmatrix},\ \delta = \begin{bmatrix} [\delta_1] \\ [\delta_2] \\ \vdots \\ \vdots \\ \vdots \\ [\delta_{J-1}] \\ [\delta_J] \end{bmatrix}, \mathrm{r} = \begin{bmatrix} [r_1] \\ [r_2] \\ \vdots \\ \vdots \\ \vdots \\ [r_{J-1}] \\ [r_J] \end{bmatrix}.$$

where

$$[A_1]=\begin{bmatrix} 0 & 0 & 1 & 0 & 0 \\ -\frac{1}{2}h_1 & 0 & 0 & -\frac{1}{2}h_1 & 0 \\ 0 & -\frac{1}{2}h_1 & 0 & 0 & -\frac{1}{2}h_1 \\ (a_2)_1 & 0 & (a_3)_1 & (a_1)_1 & 0 \\ 0 & (b_2)_1 & (b_3)_1 & 0 & (b_1)_1 \end{bmatrix}, \tag{38}$$

$$\left[A_j\right]=\begin{bmatrix} -\frac{1}{2}hj & 0 & 1 & 0 & 0 \\ -1 & 0 & 0 & -\frac{1}{2}hj & 0 \\ 0 & -1 & 0 & 0 & -\frac{1}{2}hj \\ (a_6)_j & (a_8)_j & (a_3)_j & (a_1)_j & 0 \\ (b_8)_j & (b_6)_j & (b_3)_j & 0 & (b_1)_j \end{bmatrix}, \quad 2 \le j \le J \tag{39}$$

$$\left[B_j\right]=\begin{bmatrix} 0 & 0 & -1 & 0 & 0 \\ 0 & 0 & 0 & -\frac{1}{2}h_j & 0 \\ 0 & 0 & 0 & 0 & -\frac{1}{2}h_j \\ 0 & 0 & (a_4)_j & (a_2)_j & 0 \\ 0 & 0 & (b_4)_j & 0 & (b_2)_j \end{bmatrix}, \quad 2 \le j \le J \tag{40}$$

$$\left[C_j\right]=\begin{bmatrix} -\frac{1}{2}h_j & 0 & 0 & 0 & 0 \\ 1 & 0 & 0 & 0 & 0 \\ 0 & 1 & 0 & 0 & 0 \\ (a_5)_j & (a_7)_j & 0 & 0 & 0 \\ (b_7)_j & (b_5)_j & 0 & 0 & 0 \end{bmatrix}, \quad 1 \le j \le J \tag{41}$$

$$[\delta_1]=\begin{bmatrix} \delta v_0 \\ \delta t_0 \\ \delta f_1 \\ \delta v_1 \\ \delta t_1 \end{bmatrix}, \quad [\delta_j]=\begin{bmatrix} \delta u_{j-1} \\ \delta s_{j-1} \\ \delta f_j \\ \delta v_j \\ \delta t_j \end{bmatrix}, \quad 2 \le j \le J \tag{42}$$

$$[r_j]=\begin{bmatrix}(r_1)_{j-1/2}\\(r_2)_{j-1/2}\\(r_3)_{j-1/2}\\(r_4)_{j-1/2}\\(r_5)_{j-1/2}\end{bmatrix},\qquad 1\le j\le J. \tag{43}$$

with the matrix $\boldsymbol{A}$ solve by $\boldsymbol{LU}$ method.

4. Results

The numerical computation is started in Matlab with an appropriate initial profile that satisfied the boundary conditions. The validation of the numerical method and Matlab programme codes is conducted by comparing the numerical results with the previous study. Table 2 shows a good agreement with previously reported results where the relative error ((Present result – Previous result) / Previous result) measured the precision of the present result demonstrated very small. Hence, the numerical method in this study is practically accurate and acceptable. It is worth mentioning that the comparison result is to prove the numerical method and Matlab programme codes can solve the governing equations that are considered in this study where the x is the angle of the flow position at the sphere surface. The results of the ferrofluid flow at the lower stagnation point ($x \approx 0$) are shown in graphical below.

Table 2
Comparison values of $Nu_x \,\mathrm{Re}^{-1/2}$ when $\phi = M = Nr = 0$ and $\mathrm{Pr} = 1$

x/λ	Mohamed *et al.,* [21]			Present		
	-1.0	0	1.0	-1.0	0	1.0
0°	0.7858	0.8150	0.8406	0.7858 (0.0000)	0.8149 (0.0001)	0.8406 (0.0000)
10°	0.7809	0.8103	0.8362	0.7808 (0.0001)	0.8103 (0.0000)	0.8362 (0.0000)
30°	0.7419	0.7741	0.8018	0.7421 (0.0003)	0.7744 (0.0004)	0.8021 (0.0004)
50°	0.6624	0.7032	0.7354	0.6644 (0.0030)	0.7040 (0.0011)	0.7361 (0.0010)
70°	0.5356	0.5946	0.6346	0.5347 (0.0017)	0.5943 (0.0005)	0.6360 (0.0022)
90°		0.4413	0.5071		0.4412 (0.0002)	0.5071 (0.0000)
100°		0.3284	0.4313		0.3238 (0.0140)	0.4314 (0.0002)

The crucial point out here, the velocity and temperature profile of ferrofluid flow at the lower stagnation point on sphere surface will discuss when the $\mathrm{Pr}=6.2$ (water) [13,25] in order to understand the effect of parameters that influences the ferrofluid flow on the boundary layer thickness and profiles gradient. The ferrofluid is one of the nanofluid groups, thus the ferroparticles volume fraction ϕ gives a more significant impact on the boundary layer thickness of ferrofluid flow. It is noteworthy, the zero value of parameters represent that parameter is absent from the equations. Therefore, the pure water fluid without the ferroparticles denoted by $\phi = 0$. Figure 2 shows the increment of the ferroparticles volume fraction elevates the velocity of ferrofluid flow but decrement the momentum boundary layer for both flows (assisting and opposing). According to Toghraie et al.[7], the ferroparticles volume fraction contributed to the viscosity of ferrofluid when it added to water. Their experiment result discovered viscosity of ferrofluid increase when enhancing the magnetite volume fraction but decrease with an increasing temperature. These correlations were seen in Figure 2 and 3 where the velocity of ferrofluid rise concurrently with an increase in ferrofluid temperature although an increase of magnetite volume fraction elevates the viscosity of ferrofluid as well the existence of Lorentz force and buoyancy force. As the ferroparticles volume fraction enlarging, the thermal boundary layer of both flows (assisting and opposing) are augment. The same result is also reported obtained in an experiments study by [8,9]. Theoretically, the high temperature of fluid causes the kinetic energy to increase and reduce the cohesive force simultaneously accelerate the fluid molecules. Hence, the attractive binding energy between the molecules is reduced then diminishing the viscosity of the fluid. Even though the Lorentz force tends to suppress the fluid flow and leads to a decline of ferrofluid flow velocity, but the ferrofluid behaviour change when it is heated because the magnetism of ferrofluid will lose at a high enough temperature.

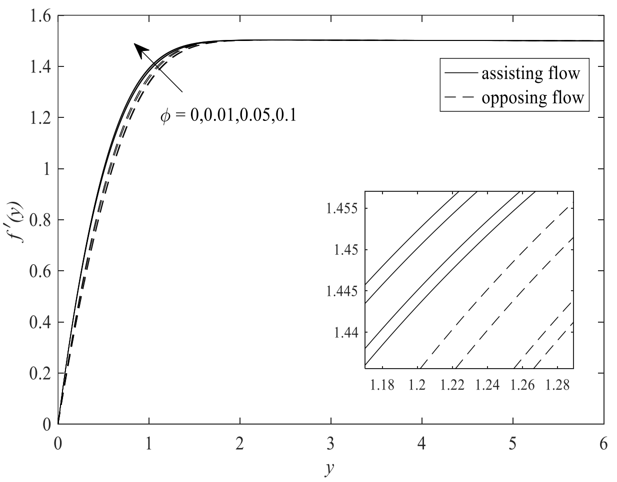

Fig. 2. Velocity profile, $f'(y)$ for different value of ϕ when $M=0.01$ and $Nr=1$

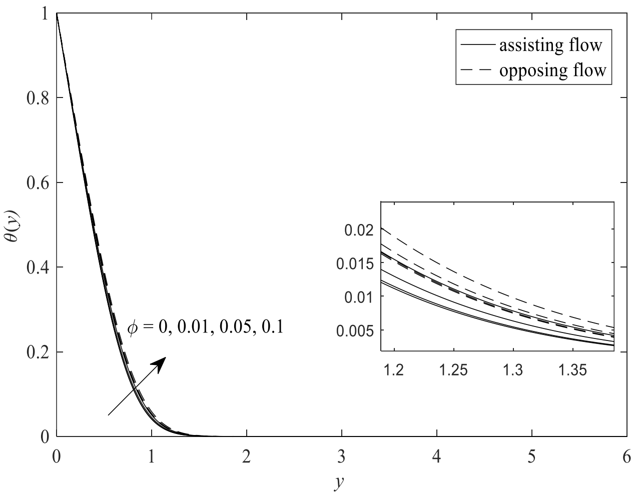

Fig. 3. Temperature profile, $\theta(y)$ for different value of ϕ when $M=0.01$ and $Nr=1$

5. Conclusions

The ferrofluid flow at lower stagnation on a sphere was scrutinized where the mixed convection heat transfer with the presence of magnetic field and thermal radiation is considered. The implementation of Keller-box method to solve partial differential equations give an impressive view of the ferrofluid flow. The random molecular motion of the ferrofluid due to the differential temperature between the fluid and sphere surface contributed to the heat transfer and change the ferrofluid flow behaviour. The numerical results revealed that the change in ferroparticles volume fraction in water considerably alter the thermophysical properties and enhance the thermal conductivity of ferrofluid. Consequently, the rate of heat transfer will improve. The increasing of the ferroparticles volume fraction leads to elevates the ferrofluid velocity and leads to a decline in the momentum boundary layer. This phenomenon is affected by the viscosity of ferrofluid that exposed to the heated surface.

Acknowledgement
The author would like to thank the Ministry of Higher Education Malaysia for providing financial support under the Fundamental Research grant (FRGS/1/2019/STG06/UMP/02/1) (University reference: RDU1901124) and Universiti Malaysia Pahang from Internal Research grant (RDU223203).

References
[1] Schlichting, Hermann. "Klaus Gersten." *Boundary-Layer Theory Ninth Edition. Verlag Berlin Heidelberg: Springer* (2017). https://doi.org/10.1007/978-3-662-52919-5
[2] Sidik, Nor Azwadi Che, H. A. Mohammed, Omer A. Alawi, and S. Samion. "A review on preparation methods and challenges of nanofluids." *International Communications in Heat and Mass Transfer* 54 (2014): 115-125. https://doi.org/10.1016/j.icheatmasstransfer.2014.03.002
[3] Rosensweig, R. E. "Ferrohydrodynamics Cambridge University Press Cambridge." *New York, Melbourne* (1985).
[4] Tsuda S, Rosensweig RE. Ferrofluid centered voice coil speaker, 2010. https://doi.org/10.1121/1.3554777
[5] Rosensweig, Ronald E., Yuki Hirota, Sayaka Tsuda, and K. Raj. "Study of audio speakers containing ferrofluid." *Journal of Physics: Condensed Matter* 20, no. 20 (2008): 204147. https://doi.org/10.1088/0953-8984/20/20/204147
[6] Scherer, Claudio, and Antonio Martins Figueiredo Neto. "Ferrofluids: properties and applications." *Brazilian journal of physics* 35, no. 3A (2005): 718-727. https://doi.org/10.1590/S0103-97332005000400018
[7] Toghraie, Davood, Seyed Mohammadbagher Alempour, and Masoud Afrand. "Experimental determination of viscosity of water based magnetite nanofluid for application in heating and cooling systems." *Journal of Magnetism and Magnetic Materials* 417 (2016): 243-248. https://doi.org/10.1016/j.jmmm.2016.05.092
[8] Malekzadeh, A., A. R. Pouranfard, N. Hatami, A. Kazemnejad Banari, and M. R. Rahimi. "Experimental Investigations on the Viscosity of Magnetic Nanofluids under the Influence of Temperature, Volume Fractions of Nanoparticles and External Magnetic Field." *Journal of Applied Fluid Mechanics* 9, no. 2 (2016). https://doi.org/10.18869/acadpub.jafm.68.225.24022
[9] Sundar, L. Syam, Manoj K. Singh, and Antonio CM Sousa. "Investigation of thermal conductivity and viscosity of Fe_3O_4 nanofluid for heat transfer applications." *International communications in heat and mass transfer* 44 (2013): 7-14. https://doi.org/10.1016/j.icheatmasstransfer.2013.02.014
[10] Colla, L., L. Fedele, M. Scattolini, and S. Bobbo. "Water-based Fe2O3 nanofluid characterization: thermal conductivity and viscosity measurements and correlation." *Advances in Mechanical Engineering* 4 (2012): 674947. https://doi.org/10.1155/2012/674947
[11] EL-Kabeir, Saber, Ahmed Rashad, Waqar Khan, and Zeinab Mahmoud Abdelrahman. "Micropolar ferrofluid flow via natural convective about a radiative isoflux sphere." *Advances in Mechanical Engineering* 13, no. 2 (2021): 1687814021994392. https://doi.org/10.1177/1687814021994392
[12] Pourhoseini, S. H., H. Ramezani-Aval, and N. Naghizadeh. "FHD and MHD effects of Fe_3O_4-water magnetic nanofluid on the enhancement of overall heat transfer coefficient of a heat exchanger." *Physica Scripta* 95, no. 4 (2020): 045705. https://doi.org/10.1088/1402-4896/ab6eb6
[13] Jamaludin, Anuar, Kohilavani Naganthran, Roslinda Nazar, and Ioan Pop. "Thermal radiation and MHD effects in the mixed convection flow of Fe_3O_4–water ferrofluid towards a nonlinearly moving surface." *Processes* 8, no. 1 (2020): 95. https://doi.org/10.3390/pr8010095
[14] Mohamed, Muhammad Khairul Anuar, Nurul Ainn Ismail, Norhamizah Hashim, Norlianah Mohd Shah, and Mohd Zuki Salleh. "MHD slip flow and heat transfer on stagnation point of a magnetite (Fe_3O_4) ferrofluid towards a stretching sheet with Newtonian heating." *CFD Letters* 11, no. 1 (2019): 17-27.
[15] Papell, S. S. "Low viscosity magnetic fluid obtained by the colloidal suspension of magnetic particles Patent." (1965).
[16] Darus, Amer Nordin. *Analisis pemindahan haba: Olakan*. Dewan Bahasa dan Pustaka, Kementerian Pendidikan Malaysia, 1995.
[17] Buongiorno, Jacopo. "Convective transport in nanofluids." (2006): 240-250. https://doi.org/10.1115/1.2150834
[18] Tiwari, Raj Kamal, and Manab Kumar Das. "Heat transfer augmentation in a two-sided lid-driven differentially heated square cavity utilizing nanofluids." *International Journal of heat and Mass transfer* 50, no. 9-10 (2007): 2002-2018. https://doi.org/10.1016/j.ijheatmasstransfer.2006.09.034
[19] Jusoh, Rahimah, Roslinda Nazar, and Ioan Pop. "Magnetohydrodynamic rotating flow and heat transfer of ferrofluid due to an exponentially permeable stretching/shrinking sheet." *Journal of Magnetism and Magnetic Materials* 465 (2018): 365-374. https://doi.org/10.1016/j.jmmm.2018.06.020

[20] Yasin, Siti Hanani Mat, Muhammad Khairul Anuar Mohamed, Zulkhibri Ismail, Basuki Widodo, and Mohd Zuki Salleh. "Numerical solution on MHD stagnation point flow in ferrofluid with Newtonian heating and thermal radiation effect." *Journal of Advanced Research in Fluid Mechanics and Thermal Sciences* 57, no. 1 (2019): 12-22.

[21] Mohamed, Muhammad Khairul Anuar, Norhafizah Mohd Sarif, N. A. Z. M. Noar, Mohd Zuki Salleh, and Anuar Ishak. "Viscous dissipation effect on the mixed convection boundary layer flow towards solid sphere." *Trans. Sci. Technol* 3 (2016): 59-67.

[22] Hussain, Shafqat, and Sameh E. Ahmed. "Unsteady MHD forced convection over a backward facing step including a rotating cylinder utilizing Fe_3O_4-water ferrofluid." *Journal of Magnetism and Magnetic Materials* 484 (2019): 356-366. https://doi.org/10.1016/j.jmmm.2019.04.040

[23] Sheikholeslami, M., and S. A. Shehzad. "Thermal radiation of ferrofluid in existence of Lorentz forces considering variable viscosity." *International Journal of Heat and Mass Transfer* 109 (2017): 82-92. https://doi.org/10.1016/j.ijheatmasstransfer.2017.01.096

[24] Malik, M. Y., T. Salahuddin, Arif Hussain, and S. Bilal. "MHD flow of tangent hyperbolic fluid over a stretching cylinder: using Keller box method." *Journal of magnetism and magnetic materials* 395 (2015): 271-276. https://doi.org/10.1016/j.jmmm.2015.07.097

[25] Sheikholeslami, Mohsen, Ahmad Arabkoohsar, Ilyas Khan, Ahmad Shafee, and Zhixiong Li. "Impact of Lorentz forces on Fe_3O_4-water ferrofluid entropy and exergy treatment within a permeable semi annulus." *Journal of cleaner production* 221 (2019): 885-898. https://doi.org/10.1016/j.jclepro.2019.02.075